

Actin remodeling by Nck regulates endothelial lumen formation

Sankar P. Chaki^a, Rola Barhoumi^b, and Gonzalo M. Rivera^a

^aDepartment of Veterinary Pathobiology and ^bDepartment of Veterinary Integrative Biosciences, Texas A&M University, College Station, TX 77843-4467

ABSTRACT Multiple angiogenic cues modulate phosphotyrosine signaling to promote vasculogenesis and angiogenesis. Despite its functional and clinical importance, how vascular cells integrate phosphotyrosine-dependent signaling to elicit cytoskeletal changes required for endothelial morphogenesis remains poorly understood. The family of Nck adaptors couples phosphotyrosine signals with actin dynamics and therefore is well positioned to orchestrate cellular processes required in vascular formation and remodeling. Culture of endothelial cells in three-dimensional collagen matrices in the presence of VEGF stimulation was combined with molecular genetics, optical imaging, and biochemistry to show that Nck-dependent actin remodeling promotes endothelial cell elongation and proper organization of VE-cadherin intercellular junctions. Major morphogenetic defects caused by abrogation of Nck signaling included loss of endothelial apical-basal polarity and impaired lumenization. Time-lapse imaging using a Förster resonance energy transfer biosensor, immunostaining with phospho-specific antibodies, and GST pull-down assays showed that Nck determines spatiotemporal patterns of Cdc42/aPKC activation during endothelial morphogenesis. Our results demonstrate that Nck acts as an important hub integrating angiogenic cues with cytoskeletal changes that enable endothelial apical-basal polarization and lumen formation. These findings point to Nck as an emergent target for effective antiangiogenic therapy.

Monitoring Editor

Jonathan Chernoff
Fox Chase Cancer Center

Received: Jun 4, 2015

Revised: Jun 30, 2015

Accepted: Jul 1, 2015

INTRODUCTION

The development of a functional vasculature involves the assembly of the primary capillary plexus, a process called vasculogenesis, and subsequent network expansion and remodeling through various mechanisms of angiogenesis (Carmeliet, 2003; Adams and Alitalo, 2007). Vascular morphogenesis is orchestrated by multiple angiogenic cues that elicit a coordinated response of endothelial cells, including proliferation, transitions in polarity states, directional migration, matrix remodeling, and lumenization (Adams and Alitalo,

2007; Iruela-Arispe and Davis, 2009; Davis et al., 2011). Cytoskeletal remodeling—in particular, actin dynamics—plays a key role in the regulation of vascular morphogenesis and homeostasis (Lamalice et al., 2007; Bayless and Johnson, 2011). Cytoskeletal remodeling also underlies the aberrant endothelial response leading to pathological angiogenesis and vascular destabilization induced by an imbalance in angiogenic cues (Weis and Cheresh, 2011).

Signals that alter tyrosine phosphorylation are primarily involved in regulation of vascular morphogenesis and vessel stability (Jeltsch et al., 2013). Phosphorylation sites resulting from activation of tyrosine kinases provide a platform for the assembly of signaling complexes through the recruitment of adaptor and scaffold proteins containing phosphotyrosine-binding modules (Machida and Mayer, 2005). The family of noncatalytic regions of tyrosine kinase (Nck) adaptor proteins; hereafter Nck), consisting of Nck1/α and Nck2/β, links tyrosine phosphorylation with downstream effectors that modulate cytoskeletal dynamics (Li et al., 2001; Buday et al., 2002). These modular adaptors, composed of three N-terminal Src homology 3 (SH3) domains and one C-terminal SH2 domain, are required for the development of mesoderm-derived embryonic structures (Bladt et al., 2003), including the cardiovascular system (Clouthier et al., 2015). We and others have shown that Nck plays an important

This article was published online ahead of print in MBoC in Press (<http://www.molbiolcell.org/cgi/doi/10.1091/mbo.E15-06-0338>) on July 8, 2015.

Address correspondence to: Gonzalo M. Rivera (grivera@cvm.tamu.edu).

Abbreviations used: aPKC, atypical protein kinase C; Cdc42, cell division control protein homologue 42; FRET, Förster resonance energy transfer; HUVEC, human umbilical vein endothelial cell; Nck, noncatalytic region of tyrosine kinase; N-WASp, neuronal Wiskott–Aldrich syndrome protein; PDXL, podocalyxin; 3D, three-dimensional; VE-cadherin, vascular endothelial cadherin; VEGF, vascular endothelial growth factor.

© 2015 Chaki et al. This article is distributed by The American Society for Cell Biology under license from the author(s). Two months after publication it is available to the public under an Attribution–Noncommercial–Share Alike 3.0 Unported Creative Commons License (<http://creativecommons.org/licenses/by-nc-sa/3.0/>).

"ASCB®," "The American Society for Cell Biology®," and "Molecular Biology of the Cell®" are registered trademarks of The American Society for Cell Biology.

role in angiogenic factor-stimulated cytoskeletal remodeling and directional migration of endothelial cells (Stoletoev *et al.*, 2001; Kiosses *et al.*, 2002; Lamalice *et al.*, 2006; Anselmi *et al.*, 2012; Chaki *et al.*, 2013). However, how Nck regulates molecular and cellular mechanisms enabling endothelial morphogenesis remains largely undetermined. Using a combination of molecular genetics and three-dimensional (3D) quantitative optical microscopy we now provide evidence that Nck regulates endothelial apical-basal polarization and lumenization through the correct localization and activation of the cell division control protein homologue 42 (Cdc42)/atypical protein kinase C (aPKC) polarity complex. These findings highlight Nck as a key molecular hub downstream of multiple angiogenic cues and potential target for the development of effective antiangiogenic therapies.

RESULTS

Nck is required for endothelial cord formation

Our previous findings showing that Nck silencing impairs front-back polarity and directional migration of endothelial cells in two dimensions (Chaki *et al.*, 2013) prompted us to examine the role of Nck in endothelial cell morphogenesis. The formation of solid cords on a planar growth factor-reduced matrix involves a cytoskeletal response resembling that of capillary morphogenesis. To manipulate the cellular levels of Nck (Supplemental Figure S1C), we used a previously validated loss-of-function approach based on the expression of short hairpin RNAs (shRNAs) that consistently induced a >50% decrease in Nck1/2 protein levels (Chaki *et al.*, 2013). As a control, we used the same silencing vector (pSuper) not expressing shRNAs (empty vector). In addition, we rescued Nck1/2-silenced cells with retroviral particles harboring an shRNA-resistant mouse Nck2 cDNA that resulted in expression levels slightly above that of the endogenous Nck (Chaki *et al.*, 2013). Results show that control cells (empty vector), but not cells expressing short hairpins targeting Nck1 and Nck2 (shNck1 and 2), developed a robust and well-interconnected network of cords (Supplemental Figure S1A). Furthermore, reexpression of shRNA-resistant Nck in Nck1/2-silenced cells restored cord formation. Quantitative analysis showed a significant ($p < 0.01$) decrease in cord length, number of branching points, and nodes in Nck-depleted (shNck1 and 2) versus control or rescued cells (Supplemental Figure S1B).

Nck is required for endothelial lumen formation

Lumenization is the process that transforms solid endothelial cords into vascular tubes, which is essential for the establishment of an efficient circulatory system. To determine more precisely how Nck regulates the program of endothelial cell morphogenesis, we performed tube formation assays in 3D collagen I matrices in the presence of vascular endothelial growth factor (VEGF) stimulation. Tube formation in 3D matrices entails matrix remodeling, endothelial cell invasion, polarization, and lumenization (Koh *et al.*, 2008b). As shown in Figure 1A, control and Nck-rescued cells formed more robust networks of interconnected tubes in collagen than did Nck-silenced cells. In addition, lumenization was only apparent in control and rescued cells, whereas mostly large intracellular vacuoles were observed in Nck-depleted cells. Quantitative image analysis demonstrated a significant ($p < 0.001$) reduction in the number of branching points (unpublished data), tube length, and lumen area (Figure 1B) in Nck-silenced versus control or rescued cells.

To gain additional morphological insights, we performed transmission electron microscopy of cells cultured in 3D collagen matrices (Figure 2). By adopting an elongated squamous morphology and displaying extended, uninterrupted cell-cell contacts, control

cells formed large tubes with well-defined lumens (Figure 2, A and B, left). In contrast, Nck-silenced cells exhibited a more-rounded appearance and far-less-extended cell-cell junctions, with inclusion of large cytoplasmic vacuoles and endocytic vesicles (Figure 2, A and B, right, and C). Typically, hollow structures formed by Nck-silenced cells showed intracellular or intercellular lumens of decreased diameter (Figure 2C). Western blot analysis performed on cell extracts collected from 3D cultures showed a decrease in Nck levels in the silenced group (Figure 2D). Collectively these results point to an essential role of Nck adaptors in endothelial tubulogenesis.

Loss of Nck disrupts the cytoskeletal architecture and the distribution of vascular endothelial cadherin

Previous studies demonstrated an essential role of vascular endothelial cadherin (VE-cadherin) and the organization of endothelial cell-to-cell adherens junctions in the establishment of endothelial polarity and vascular lumen formation (Strilic *et al.*, 2009; Lampugnani *et al.*, 2010). The phenotype exhibited by Nck-silenced endothelial cells in the present study (Figures 1 and 2) prompted us to investigate the role of Nck in the distribution of VE-cadherin and the organization of endothelial adherens junctions. First, we hypothesized that Nck is enriched at VE-cadherin cell-cell junctions. Because commercially available anti-Nck antibodies are not suitable for immunofluorescence, we resorted to expression of fluorescently tagged Nck. Thus we prepared monolayers of endothelial cells expressing Nck-enhanced yellow fluorescent protein (EYFP) and performed immunostaining of endogenous VE-cadherin and/or cortactin, an Nck binding partner and regulator of junctional actin assembly (Han *et al.*, 2014). Consistent with observations in epithelial monolayers (Han *et al.*, 2014), endogenous cortactin colocalized with junctional VE-cadherin (Supplemental Figure S2A, top). In support of our hypothesis, Nck-EYFP accumulated at VE-cadherin/cortactin-rich cell-cell junctions (Supplemental Figure S2, A and B).

In light of the foregoing findings, we hypothesized that Nck modulates junctional actin/VE-cadherin dynamics. To test this hypothesis, serum-starved, confluent monolayers of human umbilical vein endothelial cells (HUECs) were left untreated or subjected to a calcium switch assay (Zandy *et al.*, 2007) followed by staining of endogenous VE-cadherin and F-actin. Results show that Nck depletion disrupted the organization and dynamics of assembly of VE-cadherin-based cell-cell junctions (Supplemental Figure S3). Control and, to a lesser extent, Nck-rescued cells presented robust localization of VE-cadherin staining at sites of cell-cell contact that displayed an organization resembling a trabecular meshwork (Supplemental Figure S3A, top). In contrast, Nck-silenced cells exhibited decreased localization of VE-cadherin at sites of cell-cell contact and almost complete absence of the trabecular meshwork architecture. In addition, calcium switch experiments revealed that Nck-depleted cells had a slight but significant ($p < 0.05$) delay in the reassembly of cell-cell contacts compared with control or Nck-rescued cells (Supplemental Figure S3, A and B). Of note, total levels of VE-cadherin were similar in control, Nck-silenced, and Nck-rescued cells (Supplemental Figure S3C).

Next we determined the distribution of endogenous VE-cadherin and the organization of cell-cell junctions in endothelial cells undergoing morphogenesis in 3D collagen matrices (Figure 3A and Supplemental Animation S1). Whereas control and rescued cells developed tubes displaying large, patent lumens and strong accumulation of VE-cadherin at extended cell-cell contacts, Nck-depleted cells formed clusters that failed to develop into a tubular network and exhibited cytosolic accumulation and patchy distribution of VE-cadherin at cell-cell contacts. In addition, control and rescued cells

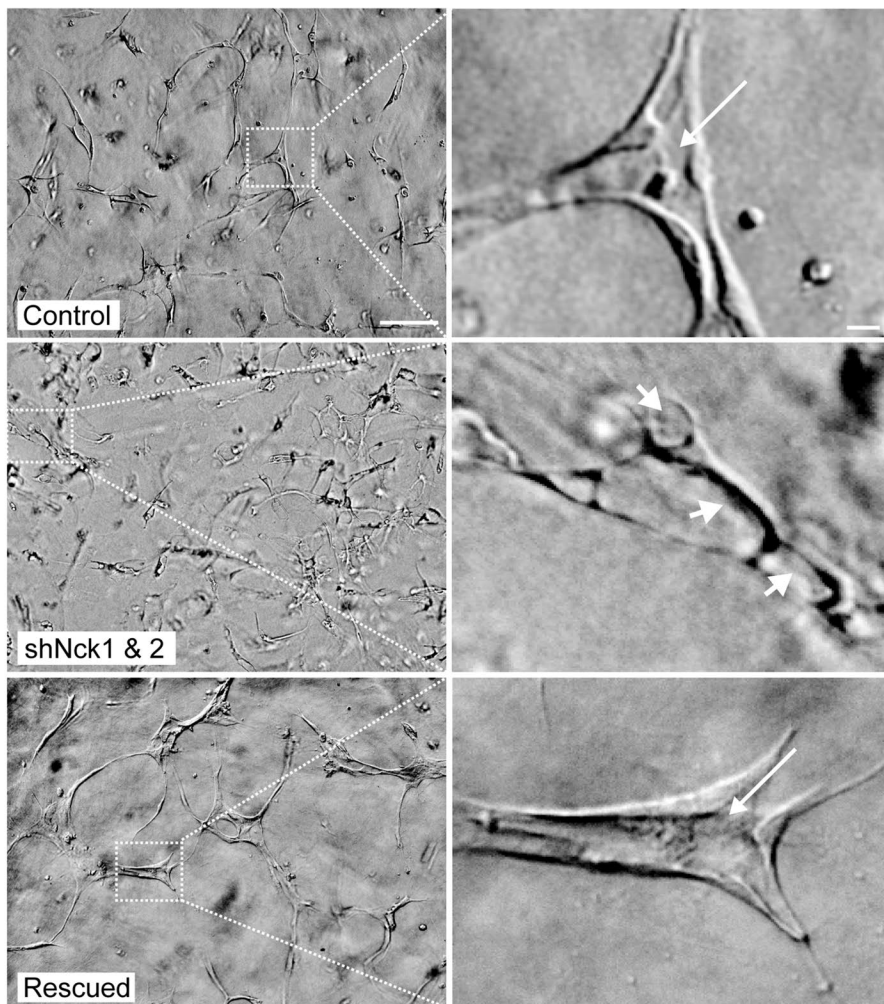
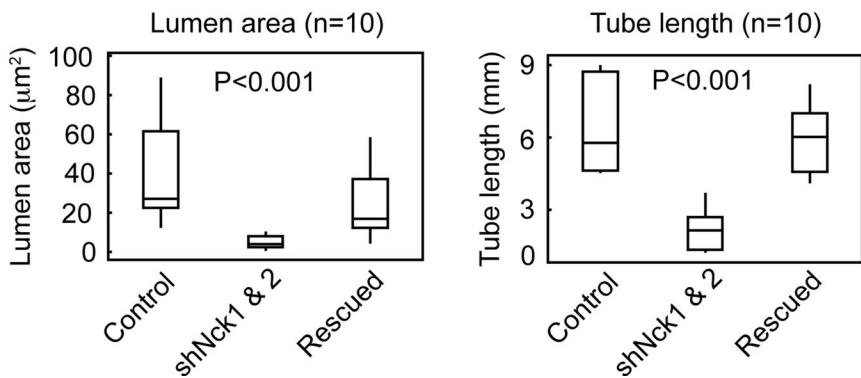
A**B**

FIGURE 1: Abrogation of Nck disrupts endothelial lumen formation in 3D collagen matrices. (A) Representative DIC images of fields (left; scale bar, 200 μm) and magnification of indicated ROIs (right; scale bar, 20 μm) from control, Nck-silenced (shNck1 and 2), and rescued cells. Arrows denote patent lumens, and arrowheads indicate intracellular vacuoles. (B) Lumen area (left) and tube length (right) in control, Nck-silenced, and rescued cells. Data derived from a total of 10 DIC fields from three independent experiments.

showed a robust cytoskeletal architecture that included long F-actin bundles delimiting extended lumens. Nck-silenced cells, in contrast, exhibited significant disruption of the cytoskeletal architecture, including the presence of F-actin aggregates and short F-actin bundles surrounding vacuolar and poorly developed hollow structures (Figure 3A and Supplemental Animation S1). Image analysis

revealed that loss of Nck induced a significant ($p < 0.001$) disruption in the cytoskeletal organization, evidenced by a reduction in the intensity of F-actin bundles, and decreased VE-cadherin accumulation at sites of cell-cell contact (Figure 3, B and C). In addition, the length of cell-cell junctions was significantly ($p < 0.001$) decreased in Nck-silenced versus control or rescued cells (Figure 3D, top). Total levels of VE-cadherin in cell extracts from 3D cultures were similar ($p > 0.05$) in control, rescued, and Nck-silenced cells (Figure 3D, bottom).

Perturbation of Nck signaling leads to loss of apical-basal endothelial polarity

Proposed mechanisms of the de novo endothelial lumen formation, that is, cord and cell hollowing, involve the vesicular delivery of fluids and membrane material to areas of cadherin-mediated cell-cell contacts (Sigurbjornsdottir et al., 2014). We hypothesized that the altered junctional VE-cadherin and cytoskeletal organization resulting from abrogation of Nck signaling leads to defective cell polarization and, consequently, incomplete lumen formation/expansion. To test this prediction, we performed immunostaining of endogenous podocalyxin (PDXL), a highly sialylated transmembrane protein involved in lumen expansion that is recruited to endothelial cell-cell contacts in a VE-cadherin-dependent manner (Strilic et al., 2009). In confluent monolayers of control and rescued HUVECs, PDXL colocalized with VE-cadherin at robust cell-cell contacts (Supplemental Figure S4A and Supplemental Animation S2). In contrast, monolayers of Nck-silenced cells showed a more diffused PDXL staining, with increased cytoplasmic and decreased junctional accumulation (Supplemental Figure S4B, top and middle). In addition, Nck-depleted but not control or rescued cells had a decreased ($p < 0.01$) junction-to-cytoplasmic PDXL ratio (Supplemental Figure S4B, bottom). Of note, the presence of PDXL/VE-cadherin-enriched cytoplasmic/membrane vesicles was readily apparent in confocal z-stacks from Nck-depleted but not control or rescued monolayers (Supplemental Figure S4A and Supplemental Animation S2). The presence of PDXL-enriched vesicles/clusters in monolayers of Nck-silenced cells was also confirmed by ground-state depletion superresolution imaging (Supplemental Figure S4C).

Next we determined the role of Nck in endothelial polarity in 3D environments. HUVECs undergoing morphogenesis in collagen I were fixed and stained with anti-PDXL, a luminal surface marker, and fluorescent phalloidin to visualize the actin cytoskeleton. In control and rescued groups, endogenous PDXL localized to luminal membranes of endothelial cells that also displayed strong actin bundles

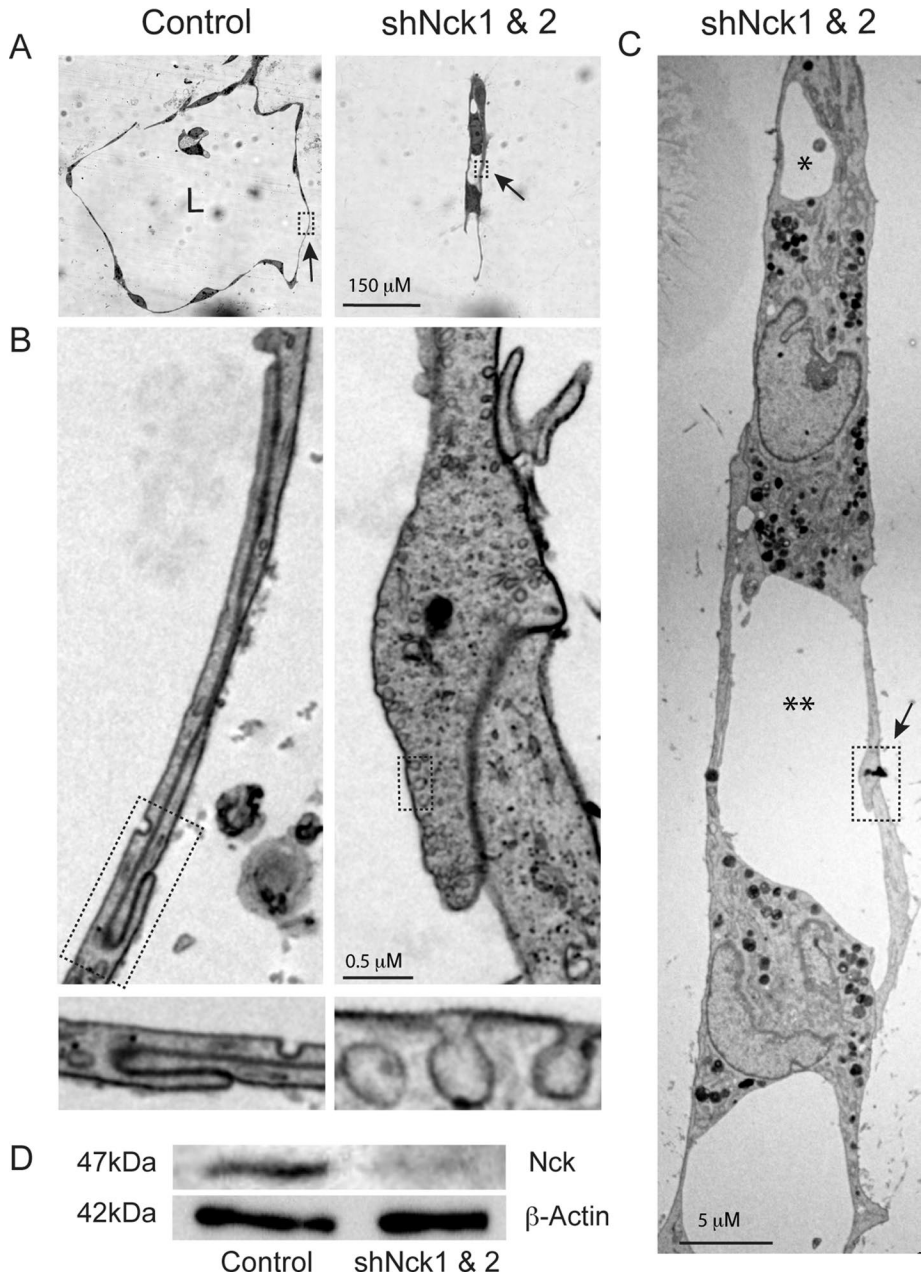


FIGURE 2: Loss of Nck impairs endothelial cell morphology in cells cultured in 3D collagen matrices. (A) Phase contrast images of 3D structures formed by control and Nck-silenced cells. (B) High-power transmission electron micrographs of ROIs indicated in A. Areas marked by rectangles are shown in greater detail at bottom. (C) Low-power transmission electron micrograph of the 3D structure formed by Nck-silenced cells shown in A. The highlighted ROI correspond to images shown in B (right). Intracellular vacuoles (*) and small lumen delimited by two cells (**) are indicated. (D) Western blot showing Nck and β -actin (loading control) levels in cell extracts from 3D cultures.

delimiting the abluminal surface of well-developed tubes (Figure 4A and Supplemental Animation S3). Line scans encompassing wall and lumens of control and rescued endothelial tubes clearly showed the polarized distribution of PDXL and actin bundles (Figure 4B). In contrast, within the small number of the 3D structures formed by Nck-silenced cells, the distribution of PDXL and the architecture of F-actin were profoundly disrupted (Figure 4, A and B). Consistent with findings in monolayers, Nck depletion led to diffuse cytoplasmic distribution and slight enrichment of PDXL in poorly developed

endothelial cell-cell contacts. Quantitative image analysis showed a significant ($p < 0.001$) decrease in the average fluorescence intensity of luminal PDXL (Figure 4C). In addition, the extent of PDXL localization to luminal region, quantified as percentage of the luminal perimeter decorated with PDXL staining, was significantly ($p < 0.001$) reduced in Nck-silenced versus control or rescued cultures (Figure 4D). The loss of PDXL polarization induced by Nck silencing was accompanied by disorganization of the architecture of actin filaments. Taken together, these findings suggest that changes in actin organization resulting from abrogation of Nck signaling contribute to loss of endothelial cell apical-basal polarity and deficient lumen formation.

Nck drives endothelial polarity and lumen formation through activation of Cdc42

To ascertain the mechanism by which Nck regulates endothelial polarity and tube morphogenesis, we determined patterns of Cdc42 activation in cells undergoing morphogenesis in 3D collagen matrices. First, the status of endogenous Cdc42 activation was ascertained using an antibody that recognizes the GTP-bound, active form of Cdc42 (Baschieri et al., 2014). In contrast to the strong luminal localization of endogenous GTP-bound Cdc42 in control and rescued cells, active Cdc42 staining was greatly decreased and distributed diffusively through the cytoplasm in Nck silenced cells (Figure 5A and Supplemental Animation S4). Remarkably, small lumens occasionally formed by Nck-knockdown cells showed almost complete absence of active Cdc42. As previously noted, the loss of Nck lead to disruption of the architecture of actin filaments. Line scans across sections of 3D cultures showed unpolarized distribution and greatly decreased overall intensity of active Cdc42 staining in Nck-silenced versus control/rescued cells (Figure 5B). Quantitative image analysis showed a significant ($p < 0.01$) decrease in the average fluorescence intensity of luminal active Cdc42 (Figure 5C). To further assess the role of Nck in the activation of Cdc42, we performed pull-down assays of endogenous GTP-bound Cdc42 in cell

extracts obtained from 3D cultures (Koh et al., 2008b) using immobilized Pak1 PBD domains (Benard and Bokoch, 2002). Consistent with the immunostaining findings, active/GTP-bound but not total Cdc42 was reduced ($p < 0.05$) in cell extracts from Nck-silenced cells compared to control or rescued cells (Figure 5, D and E).

To determine spatiotemporal patterns of Cdc42 activation in 3D cultures, we performed time-lapse confocal imaging of endothelial cells stably expressing the Raichu Cdc42 Förster resonance energy transfer (FRET) probe (Hirata et al., 2012). In contrast to

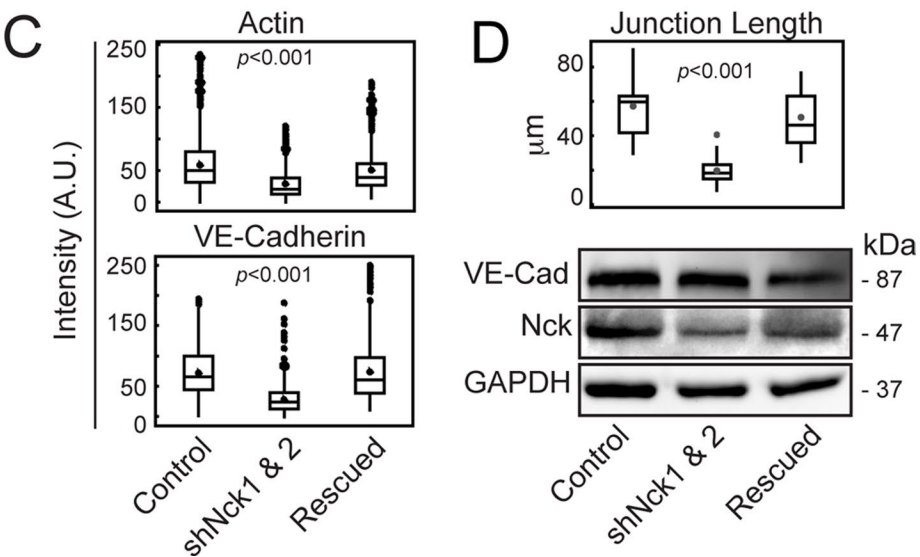
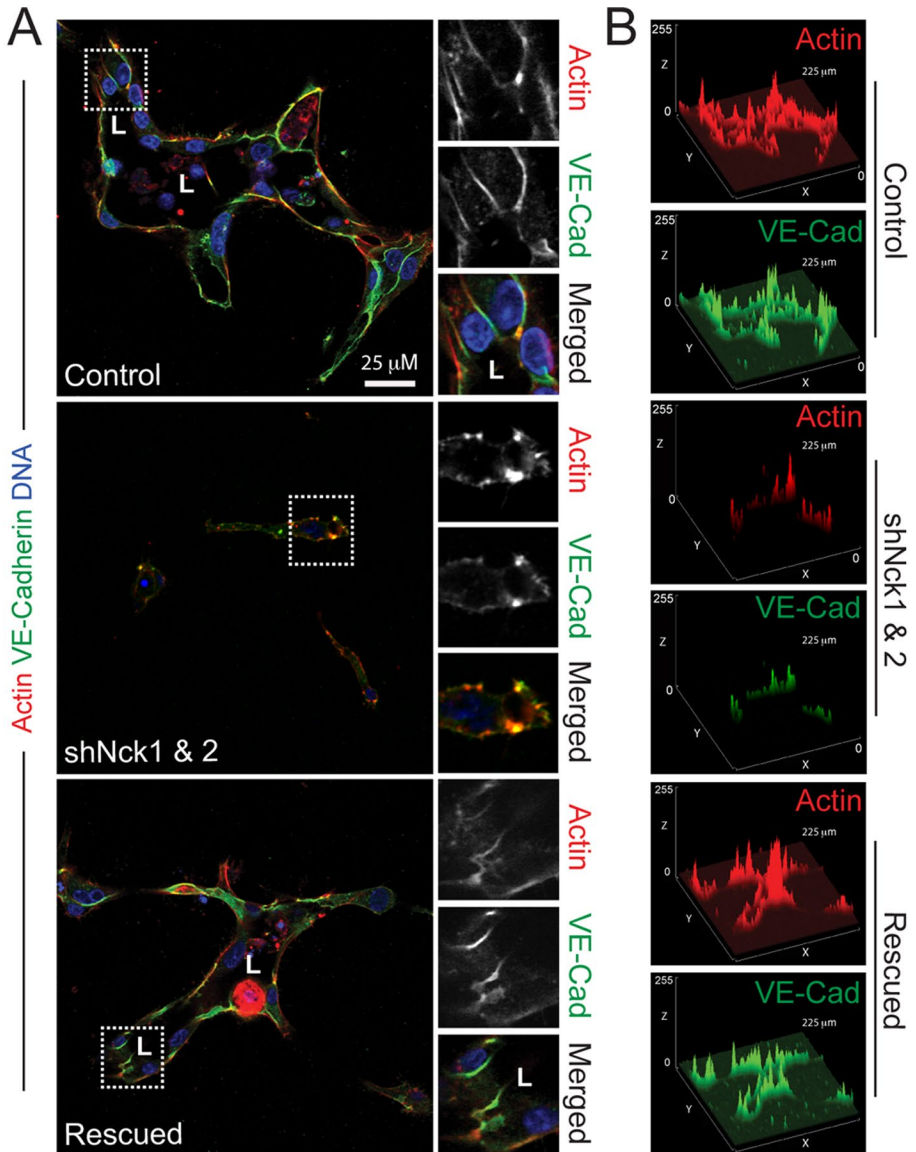


FIGURE 3: Silencing of Nck disrupts the organization of F-actin and the distribution of VE-cadherin in cells cultured in 3D collagen matrices. (A) Confocal images showing F-actin (red), endogenous VE-cadherin (green), and nuclei (blue). Lumens (L) are indicated. The ROIs (dotted

the robust activation of Cdc42 observed in cultures of control and rescued cells, the overall Cdc42 activation was significantly decreased in Nck-silenced cells (Figure 6, A and B). Compared to Nck-depleted cells, control and rescued cells showed more polarized Cdc42 activation, as evidenced by the progressive increase in FRET/teal fluorescent protein (TFP) signal from the abluminal to the luminal membrane (Figure 6, A and C). A striking association between localized Cdc42 activation and lumen expansion was present in control and rescued but not Nck-silenced cells (Supplemental Movie S1).

Nck-dependent endothelial lumenization involves activation of aPKC

The aPKC isoforms PKC ζ and PKC γ/λ form a stable complex with Par6 and contribute to the establishment of polarity by binding Par3, which, in turn, interacts with proteins of the junctional complex (Rosse et al., 2010). Previous studies showed that disruption of the Cdc42-Par3-Par6-aPKC polarity complex leads to impaired endothelial cell lumen and tube formation in 3D collagen matrices (Bayless and Davis, 2002; Koh et al., 2008a). Thus, to ascertain the contribution of Nck to the spatial regulation of aPKC activation during endothelial morphogenesis, we performed immunostaining of endogenous, phosphorylated aPKC (p-aPKC) using an antibody that recognizes phosphorylated aPKC ζ (phospho-T410) and aPKC γ/λ (phospho-T412). Consistent with spatial patterns of Cdc42 activation, strongly polarized p-aPKC staining was observed in control and rescued endothelial tubes (Figure 7, A and B). As shown in Supplemental Animation S5, control and rescued tubes typically displayed intense luminal p-aPKC signal along with well-organized abluminal F-actin bundles. In contrast, structures formed by Nck-silenced cells

(squares) were magnified and are shown to the right. (B) Surface plots showing pixel intensities for field images in A. (C) Actin and VE-cadherin accumulation at cell-cell contacts. Mean fluorescence intensity was quantified in 23–50 equal-size ROIs pooled from three independent experiments. (D) Quantitation of VE-cadherin cell-cell junctional lengths (top). Data represent mean junctional length (μm) determined in a total of 25–30 junctions pooled from three individual experiments. The Western blots (bottom) show the levels of VE-cadherin, Nck, and GAPDH (loading control) in cell extracts from 3D cultures.

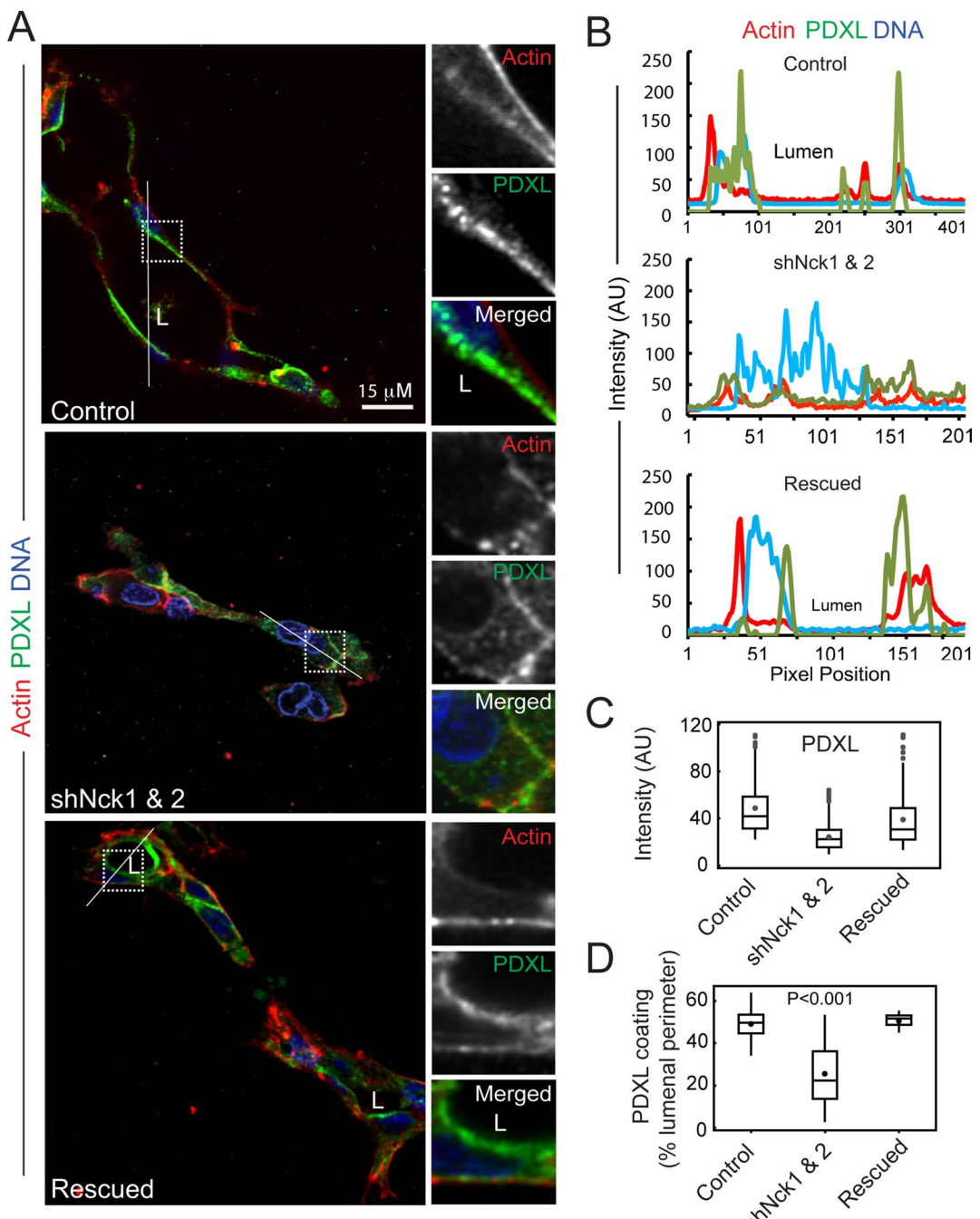


FIGURE 4: Nck regulates endothelial polarity and lumen formation in cells cultured in 3D collagen matrices. (A) Confocal images showing the cytoskeletal architecture (F-actin; red), distribution of endogenous podocalyxin (PDXL; green), and nuclei (DNA; blue). Lumens (L) are indicated. The ROIs (dotted squares) were magnified and are shown to the right. (B) Line scans showing intensities along the solid white lines displayed in A. (C) Average luminal PDXL fluorescence intensity. From 35 to 50 luminal ROIs from images collected in three independent experiments were included in the analysis. (D) Percentage of the luminal perimeter decorated with PDXL staining. From 25 to 30 lumens from images collected in three independent experiments were analyzed.

showed diffuse (unpolarized) and significantly decreased overall p-aPKC staining. Quantitative image analysis showed a significant decrease in the average fluorescence intensity of luminal p-aPKC in Nck-silencing versus control and rescued cells (Figure 7C). Consistent with these findings, levels of phosphorylated (active) aPKC, determined by Western blotting, were significantly decreased in extracts from 3D cultures of Nck-silenced cells compared to control or rescued cells (Figure 7D). Collectively these results show a key

role for Nck in the establishment of endothelial apical-basal polarity and lumen formation through a mechanism that involves spatiotemporal regulation of the Cdc42/aPKC polarity complex.

DISCUSSION

The present study provides evidence that Nck, a family of multidomain adaptors, plays an essential role in the coordination of key cellular behaviors during endothelial morphogenesis. We show that

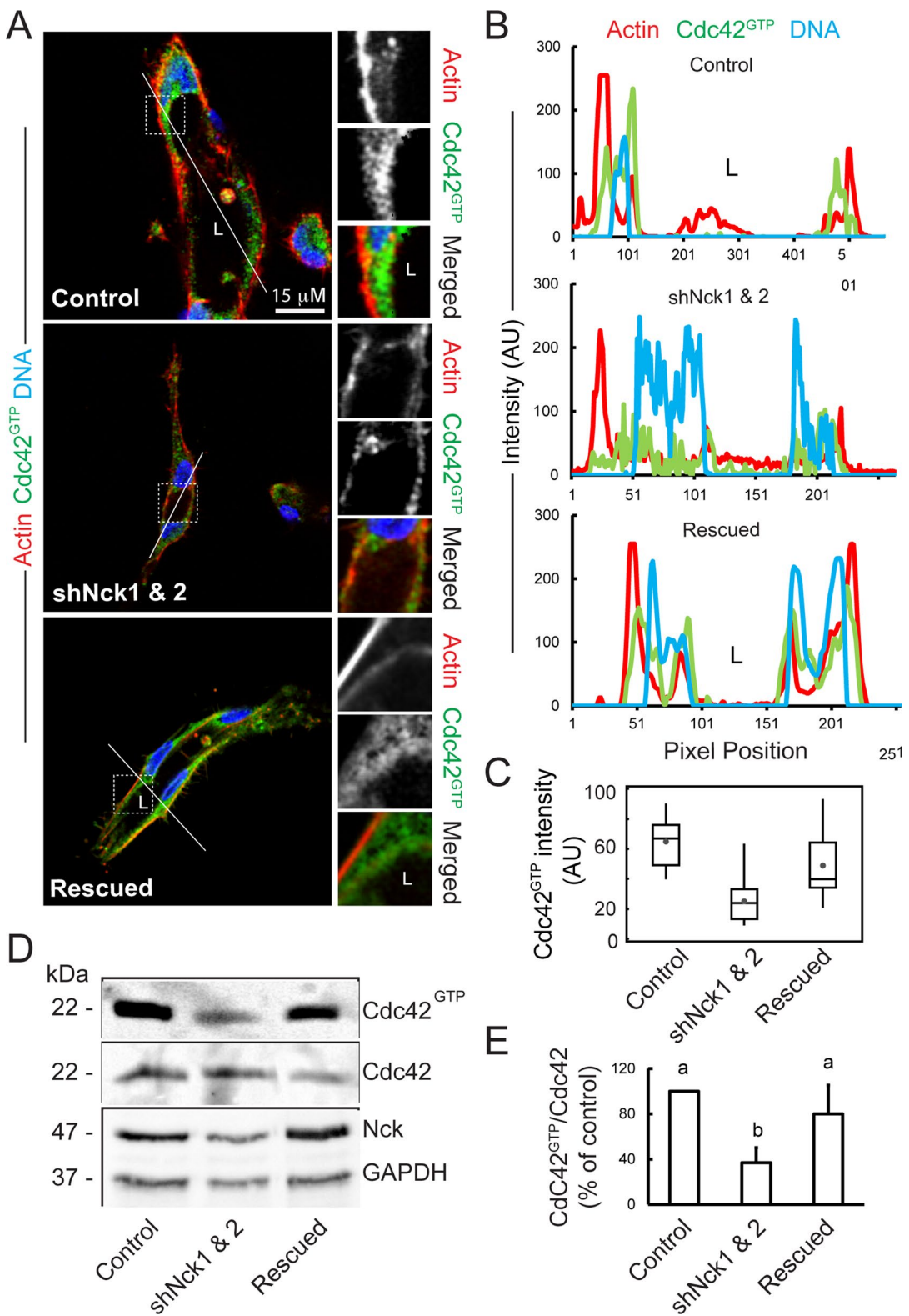


FIGURE 5: Loss of Nck disrupts activation of endogenous Cdc42 in cells cultured in 3D collagen matrices. (A) Confocal images showing the cytoskeletal architecture (F-actin; red), distribution of GTP-bound Cdc42 (Cdc42^{GTP}; green), and nuclei (DNA; blue). Lumens (L) are indicated. The ROIs (dotted squares) were magnified and are shown to the right. Scale bar, 15 μ m. (B) Line scans showing intensities along the solid white lines displayed in A. (C) Quantification of luminal Cdc42 fluorescence intensity. Average pixel intensity was extracted from 35–50 ROIs from images acquired in three independent experiments. (D) Representative Western blots showing levels of GTP-bound Cdc42 (PBD^{Pak1} pull-down assays), total Cdc42, Nck, and GAPDH in cell extracts obtained from 3D cultures. (E) Quantification of active Cdc42. The intensity of bands corresponding to active Cdc42 (PBD^{Pak1} pull-down assays) was normalized by the intensity of bands corresponding to total Cdc42 in cell extracts and expressed as percentage of control cultures ($n = 3$ independent experiments).

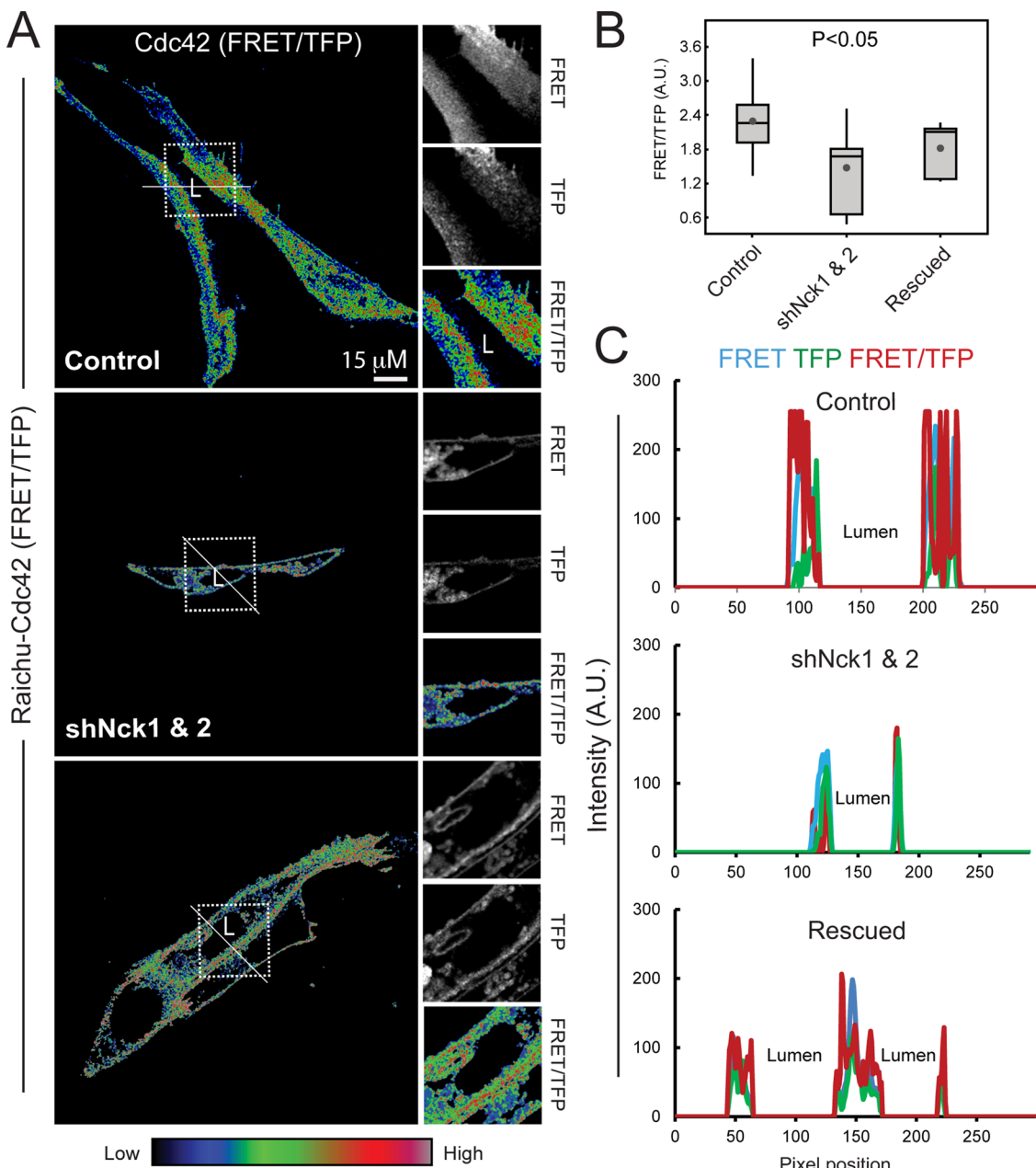


FIGURE 6: Nck modulates the spatiotemporal activation of Cdc42 in endothelial cells cultured in 3D collagen matrices. (A) FRET/TFP ratio images selected from time-lapse series of 3D cultures of HUVECs expressing the Raichu-Cdc42 FRET biosensor. The ROIs (dotted squares) were magnified and are shown to the right. The images represent FRET activity coded by the color scale (red, high activity; blue, low activity). (B) Activity of the Raichu-Cdc42 FRET probe (whole fields) from time-lapse sequences ($n = 4\text{--}6$ cells/condition from each of three independent experiments). (C) Line scans showing intensities along the solid white lines in the field images shown in A.

abrogation of Nck disrupts the architectural organization of the actin cytoskeleton and VE-cadherin junctions, resulting in loss of endothelial apical-basal polarity and impaired lumen formation. Through the combination of 3D live-cell imaging and biochemistry, this study highlights new mechanistic insights by which Nck modulates the spatiotemporal activation of the Cdc42/aPKC polarity complex. These findings are consistent with current views that, rather than simple docking or molecular linkers, adaptor proteins integrate and specify the flow of information in signaling networks by dynamically engaging distinct interaction partners at specific subcellular locations, promoting cooperative binding and clustering signaling

effectors (Pawson, 2007; Good et al., 2011). The present findings support the hypothesis that Nck acts as a hub integrating signals driving endothelial morphogenesis.

Requirement of Nck in endothelial morphogenesis

Bladt et al. (2003) described profound developmental defects in mesoderm-derived tissues and embryonic lethality in mice caused by inactivation of Nck (both Nck1 and Nck2). Similarly, findings from a recent study showed that constitutive deletion of Nck in the endothelium of mice results in impaired cardiovascular development and embryonic lethality (Clouthier et al., 2015). Although the study by

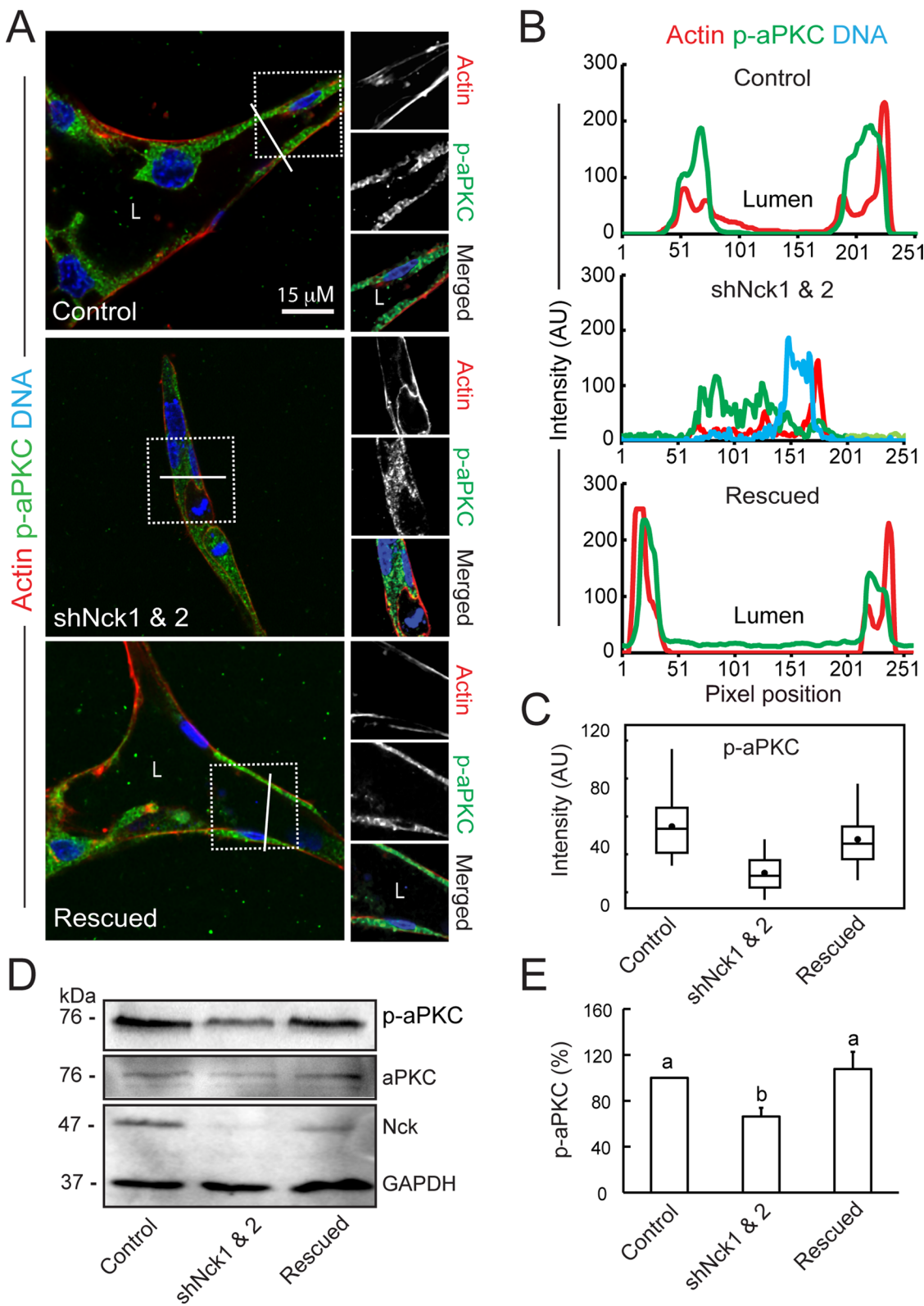


FIGURE 7: Loss of Nck disrupts the activation of endogenous aPKC in cells cultured in 3D collagen matrices.

(A) Confocal images showing the cytoskeletal architecture (F-actin; red), distribution of active aPKC (p-aPKC; green), and nuclei (DNA; blue). Lumens (L) are indicated. The ROIs (dotted squares) were magnified and are shown to the right. (B) Line scans showing intensities along the solid white lines displayed in A. (C) Quantification of luminal p-aPKC fluorescence intensity. Average pixel intensity was extracted from 35–50 ROIs from images acquired in three independent experiments. (D) Representative Western blots showing levels of p-aPKC, total aPKC, Nck, and GAPDH in cell extracts from 3D cultures. (E) Quantification of active aPKC. The intensity of bands corresponding to p-aPKC was normalized by the intensity of bands corresponding to total aPKC and expressed as percentage of control cultures ($n = 3$ independent experiments). a, b, $p < 0.05$.

Clouthier et al. (2015) established that Nck is required for endothelial tip cell sprouting, insights into the precise role of Nck in the regulation of angiogenesis were limited by early embryonic lethality.

We and others have shown that Nck plays an important role in angiogenic factor-stimulated cytoskeletal remodeling and directional migration of endothelial cells (Stoletov et al., 2001; Kiosses et al., 2002; Lamalice et al., 2006; Chaki et al., 2013). However, the cellular mechanisms underlying Nck-regulated endothelial morphogenesis have remained largely unknown. Our present findings disclose new links between Nck-mediated actin remodeling and key cellular mechanisms necessary for endothelial lumen formation, including intercellular junctional elongation and apical-basal polarization. Remarkably, Nck silencing suppressed lumen formation or resulted in intracellular vacuoles/small luminal structures that fail to coalesce and/or expand. We speculate that Nck contributes to endothelial lumenization through regulation of the fusogenic, adhesion, and matrix-remodeling machineries of endothelial cells.

Loss of Nck disrupts actin and the organization of VE-cadherin cell–cell junctions

VE-cadherin cell–cell adhesion is required for vascular morphogenesis and stabilization (Montero-Balaguer et al., 2009). Dynamics of actin filaments and endothelial adherens junctions are reciprocally regulated (Abu Taha et al., 2014). Here we provide evidence that Nck silencing results in altered endothelial cell morphology, disorganization of the actin cytoskeleton, and disruption of VE-cadherin cell–cell junctions. This is consistent with recent findings in zebrafish showing that VE-cadherin ablation impairs actin polymerization, stalk cell elongation, and the extension of the endothelial cell–cell interface (Sauteur et al., 2014). Given that pharmacological inhibition of actin polymerization phenocopies the junctional defects resulting from VE-cadherin deletion (Sauteur et al., 2014), it is possible that localized actin polymerization stimulated by Nck promotes junction elongation.

Arp2/3-dependent actin nucleation and filament stabilization are involved in the formation of cortical actin rings that support intercellular junctional organization (Kovacs et al., 2011; Abu Taha et al., 2014). Arp2/3-dependent actin polymerization at endothelial cell–cell junctions is promoted by the nucleation-promoting factors neuronal Wiskott-Aldrich syndrome protein (N-WASp; Rajput et al., 2013) and cortactin (Boguslavsky et al., 2007; Han et al., 2014). In vitro, Nck forms a complex with cortactin and WIP/N-WASp that stimulates Arp2/3-dependent actin polymerization (Tehrani et al., 2007). In living cells, we demonstrated that clustering of Nck stimulates Arp2/3-stimulated actin polymerization through the activation of WIP/N-WASp (Rivera et al., 2004; Ditlev et al., 2012). Thus the present findings showing that Nck colocalizes with cortactin at VE-cadherin cell–cell junctions support the hypothesis that Nck plays a key role in polymerization/stabilization of junctional actin filaments through the cortactin/N-WASp/Arp2/3 axis. Interestingly, zonula occludens (ZO-1), a protein that bridges the cadherin/catenin complex and junctional actin filaments (Itoh et al., 1997), is required for normal cadherin-dependent actin organization during development (Lockwood et al., 2008). Because ZO-1 is recruited to actin filaments induced by membrane-targeted Nck (Hanajima-Ozawa et al., 2007), it represents a plausible link between endothelial adherens junction dynamics and Nck-dependent actin remodeling.

Loss of Nck disrupts endothelial polarity and lumen formation

Depending on vessel type/cellular context, distinct cellular mechanisms are used alternatively or in combination during vascular lumen

formation (Davis and Camarillo, 1996; Kamei et al., 2006; Herbert et al., 2009; Strilic et al., 2009; Herwig et al., 2011). Nonetheless, the establishment of endothelial apical-basal polarity is believed to be a prerequisite for endothelial lumenization. Among various molecular players, $\beta 1$ integrin (Zovein et al., 2010) and VE-cadherin (Lampugnani et al., 2010) have been identified as key drivers of endothelial polarity and lumen formation. Both $\beta 1$ integrin and VE-cadherin coordinate the recruitment of actin filaments and apical proteins, including sialomucins, to the incipient endothelial lumen (Strilic et al., 2009; Zovein et al., 2010). Remarkably, the disruption of junctional VE-cadherin and F-actin organization induced by Nck silencing caused delocalization of the sialomucin PDXL and loss of apical-basal endothelial polarity. Accordingly, Nck silencing resulted in negligible luminal formation or the formation of intracellular vacuoles and intercellular luminal structures that failed to coalesce/expand. Thus we propose that Nck promotes endothelial cell interface elongation by a mechanism that involves localized actin polymerization/stabilization and, consequently, the organization of junctional VE-cadherin.

Coordination and interdependence of cadherin and integrin adhesions, the “adhesive cross-talk,” is mediated by convergent signaling mediated by shared effectors, including adaptors/scaffolds and Rho GTPases (Weber et al., 2011). For example, a recent study showed that integrin $\beta 1$ function is required for proper localization of VE-cadherin, endothelial cell–cell junction integrity, and the formation of stable, nonleaky blood vessels through a mechanism that involves RhoA and Rap1 activation (Yamamoto et al., 2015). Of interest, mouse embryos lacking endothelial Nck showed compromised vascular integrity, including increased edema and profuse hemorrhages (Clouthier et al., 2015). We showed previously that Nck modulates integrin $\alpha 5\beta 1$ -extracellular matrix adhesion force and endothelial cell stiffness by regulating the activation of RhoA (Chaki et al., 2013). Collectively these findings suggest that Nck integrates signaling networks responsive to cell–cell and cell–matrix cues.

Nck drives endothelial polarity and lumenization through Cdc42/aPKC

The Rho GTPases—molecular switches that regulate cytoskeletal dynamics (Hall, 2012)—are major determinants of cell polarity (Roignot et al., 2013; Rodriguez-Boulan and Macara, 2014). In particular, Cdc42 (Bayless and Davis, 2002; Koh et al., 2008a; Qi et al., 2011; Jin et al., 2013; Liu et al., 2013) and its effector the Par3/Par6/aPKC complex (Kamei et al., 2006; Koh et al., 2008a; Qi et al., 2011) are required for endothelial lumen formation. Here we demonstrate that Nck specifies spatiotemporal patterns of Cdc42/aPKC activation during endothelial morphogenesis. Previous studies documented the cooperation between Nck and Cdc42 in the activation of N-WASp-stimulated actin polymerization (Dart et al., 2012; Humphries et al., 2014). Further, the Cdc42/Par6/aPKC polarity axis was shown to regulate adherens junction stability through modulation of N-WASp/Arp2/3-dependent actin remodeling (Georgiou et al., 2008). Because Nck stimulates N-WASp/Arp2/3-dependent actin polymerization (Rivera et al., 2004; Ditlev et al., 2012), we postulate that Nck modulates morphogenesis by linking spatiotemporally restricted activation of Cdc42-dependent polarity signals, junctional actin polymerization, and VE-cadherin adhesion dynamics. Given its significant role in signaling downstream of integrin (Tu et al., 1998; Goicoechea et al., 2002; Vaynberg et al., 2005), VEGF (Stoletov et al., 2001; Lamalice et al., 2006), and guidance receptors (Cheng et al., 2002; Li et al., 2002; Fan et al., 2003; Miura et al., 2009), the Nck hub appears uniquely

positioned to coordinate key cellular processes during vascular morphogenesis.

MATERIALS AND METHODS

Reagents

HUVECs, EBM2/EGM2 culture medium, Hank's balanced salt solution, trypsin-EDTA, and trypsin neutralizing solution were purchased from Lonza (Walkersville, MD). Other reagents were purchased from the following sources: DAPI (Sigma-Aldrich, St. Louis, MO), Hoechst33342 (Life Technologies, Eugene, OR), fibronectin (EMD Millipore, Billerica, MA), recombinant human VEGF 165 (R&D Systems, Minneapolis, MN), Matrigel (BD Biosciences, Sparks, MD), Texas Red phalloidin (Life Technologies), lipofectamine 2000 (Life Technologies), DMEM (HyClone, Logan, UT), fetal bovine serum (Gemini Bio-Products, West Sacramento, CA), Alexa Fluor 488 protein labeling kit (Life Technologies), anti-pPKCzeta/lambda (Abcam, Cambridge, MA), anti-VE-Cadherin (Affymetrix, Santa Clara, CA), anti-active Cdc42 (NewEast Biosciences, Malvern, PA), and anti-human podocalyxin (R&D Systems), Collagen I (Corning, Discovery Labware, Bedford, MA).

Viral production

The production of viral particles harboring vectors for the expression of shRNA or cDNA was previously described (Chaki et al., 2013). Briefly, retroviruses for the stable expression of shRNAs or cDNAs were generated in HEK293T cells by calcium phosphate precipitation. For protein silencing, the pSUPER retroviral vector carrying oligonucleotide sequences for the expression of shRNAs was used. The shRNA targeting sequences (Nck1: GAGAGAGAG-GATGAATTAT; Nck2: AACTACGTGGTGGTCCTCAGT) were previously validated (Chaki et al., 2013). For protein expression, the PMSCV retroviral vector carrying cDNAs of interest with or without fluorescent marker was used. Retroviral vectors were cotransfected with pHCMV-G and pMD.gag.pol plasmids. Medium containing virus was harvested within 48 h of transfection and stored at -80°C in aliquots for later use.

Cord network formation

For endothelial cord network formation on laminin-rich matrices, we used serum-starved (6 h) HUVECs. Cells were resuspended in EBM2 starvation medium supplemented with 50 ng/ml VEGF. Cells (2×10^4) were seeded in 96-well plates coated with a thick layer (50 μ l/well) of Matrigel and incubated for 16 h at 37°C. After fixation in paraformaldehyde (4% for 10 min) and staining in toluidine blue, cultures were subjected to bright-field imaging.

Three-dimensional, collagen-I-based vasculogenesis assay

Endothelial tube formation in 3D collagen matrices was performed following a protocol previously described (Koh et al., 2008b; Kim et al., 2013). Briefly, endothelial cells were mixed with 2–3.5 mg/ml type I collagen containing 16 nM phorbol-12-myristate-13-acetate and 1.25 μ M sphingosin-1-phosphate on ice. Subsequently, 50 μ l of cell-collagen mixture was added on 96-well glass-bottom plates and incubated at 37°C/CO₂ for 45 min to allow gel formation. A total of 100 μ l of EGM2 complete media supplemented with 50 ng/ml VEGF was added on top of the solidified collagen gel, and cultures were maintained in the incubator for 96 h.

Microscopy

Bright-field images and differential interference contrast (DIC) images were captured using an Olympus IX70 inverted micro-

scope. Confocal images were collected on a Zeiss LSM 510 Meta confocal microscope equipped with a Plan-Neofluar 40 \times /1.3 oil objective. Time-lapse series of HUVECs expressing the single-chain Raichu/Cdc42 FRET probe (Aoki and Matsuda, 2009) were collected every 1 min for 30–60 min on a Zeiss LSM 780 confocal microscope equipped with Plan-Neofluar 40 \times /1.4 oil objective. Images were collected every minute for a total of 30–60 min. For ultrastructural analysis, collagen gels were prepared for transmission electron microscopy (TEM). Briefly, gels were fixed with 2.5% glutaraldehyde and 2% paraformaldehyde in 75 mM phosphate-buffered saline (PBS) for 3 h at 4°C, followed by overnight wash in 114 mM PBS. Gels were subsequently postfixed in 1% OsO₄ reduced with 1% K₄[Fe(CN)₆] in 1 M cacodylate buffer for 1 h at 4°C, washed twice in 0.1 M cacodylate buffer, and embedded in Epon. Ultrathin sections were cut, mounted onto copper grids, and viewed with a Morgagni 268 transmission electron microscope (FEI). Digital images were acquired with a MegaViewIII camera controlled with iTEM software (Olympus Soft Imaging Systems, Germany) and then postprocessed using ImageJ (National Institutes of Health, Bethesda, MD) and Adobe Illustrator.

Image processing and analysis

Fiji was used for image processing and extraction of quantitative data. For quantitative analysis of VE-cadherin, PDXL, active Cdc42, and p-aPKC, the average fluorescence intensity in regions of interest (ROIs) located in the luminal area was measured using ImageJ software. A total of 35–50 ROIs from 3D images pooled from three independent experiments was analyzed. To determine VE-cadherin junctional length and the percentage of luminal perimeter coated with PDXL, the line scan function of ImageJ was used on 25–30 junctions/lumens from three independent experiments. Images from FRET time-lapse series were processed with Fiji. Briefly, a binary mask was derived from the YFP image and was multiplied separately with the TFP and FRET images. Then FRET images were divided by TFP images to obtain FRET/TFP ratio images. A rainbow color LUT was applied, and brightness and contrast were adjusted to display the ratio FRET images in an intensity-modulated manner by which red indicates high and blue indicates low FRET efficiency, respectively. For quantitative analysis, YFP-masked FRET and TFP images were thresholded to measure pixel intensity of each individual image in the stack, and FRET/TFP intensity ratios were calculated as previously described (Chaki et al., 2013). For statistical purposes, time-lapse series were acquired from four to six cells/group. Experiments were repeated three times.

Calcium switch assay and immunofluorescence staining

HUVECs serum starved for 10 h in EBM2 (Lonza) starvation medium containing 0.2% fetal bovine serum were challenged with 4 mM ethylene glycol tetraacetic acid (EGTA) for 30 min to chelate extracellular calcium and disrupt Ca²⁺-dependent intercellular junctions. After washing, cells were allowed to recover in calcium-containing EBM2 complete culture medium for various intervals. Cells were fixed and permeabilized with 3.7% paraformaldehyde and 0.25% Triton X-100 in cytoskeletal buffer (10 mM 2-(*N*-morpholino)ethanesulfonic acid, 150 mM NaCl, 5 mM EGTA, 5 mM MgCl₂, and 5 mM glucose (pH 6.1) for 10 min at room temperature and subsequently processed for immunofluorescence.

Immune detection of endogenous proteins was performed as previously described (Rivera et al., 2004). After fixation and permeabilization, endothelial monolayers were blocked with 2% bovine

serum albumin (BSA) in PBS (1 h) before overnight incubation with primary antibody (rabbit polyclonal anti-VE-cadherin antibody, 1:1000 [2012-02; Bender Med System], and anti-human podocalyxin antibody, 1:500 [AF 1658; R&D Systems]). Cells were then extensively washed to remove the unbound excess primary antibody and subsequently incubated with goat anti-rabbit immunoglobulin G (IgG)-horseradish peroxidase (HRP; 1:1000; sc-2054; Santa Cruz Biotechnology) containing DAPI (5 ng/ml) and Texas red phalloidin (1:100; Invitrogen) for 1 h.

Cells in 3D cultures were processed for immunofluorescence following a protocol previously described (Lampugnani et al., 2010). Briefly, after 96 h of culture, cell nuclei were stained with 50 μ l of NuBlue (Hoechst 33342) for 1 h at 37°C. Collagen gels were fixed in 3.7% paraformaldehyde for 35 min and quenched in 75 mM NH₄Cl and 20 mM glycine in PBS, pH 8.0, for 60 min. Cells were blocked in 0.7% species-specific serum (secondary antibody) and 0.3% Triton X-100 PBS (blocking buffer) for 30 min. Primary (1:50) and secondary (1:200) antibodies were incubated overnight at 4°C in blocking buffer. After 3x gentle washing in PBS, gels were kept wet with filtered 100 μ l of PBS containing 0.2% sodium azide and stored at 4°C covered with foil until imaged.

Cdc42 pull-down assay

Cells were cultured for 96 h in 3D collagen matrices, and GTP-loaded Cdc42 from cell extracts was enriched by pull down with immobilized PBD domains from Pak1 (Kutys and Yamada, 2014). Briefly, endothelial cells were lysed by sonication in ice-cold lysis buffer containing 20 mM 4-(2-hydroxyethyl)-1-piperazineethanesulfonic acid (HEPES), pH 7.6, 1% Triton X-100, 150 mM NaCl, 5 mM MgCl₂, 1 mM dithiothreitol (DTT), Sigma-Aldrich protease and phosphatase inhibitor cocktail, and 5% glycerol. After high-speed centrifugation for 10 min at 4°C, supernatants were collected and protein concentration determined by the Bradford method. Next 500 μ g of protein was incubated in the presence of 40 μ g of PBD_{Pak1}-glutathione S-transferase protein beads (Cytoskeleton) for 1 h at 4°C. Beads were washed twice with 500 μ l of ice-cold wash buffer (25 mM Tris-HCl, pH 7.5, 30 mM MgCl₂, 40 mM NaCl, 1 mM DTT, 1 mM phenylmethylsulfonyl fluoride (PMSF), 5 μ g/ml aprotinin, and 1 μ g/ml leupeptin) and boiled in sample buffer (40 μ l of beads in wash buffer plus 10 μ l of 5x sample buffer) for 5 min. Samples were resolved by SDS-PAGE, followed by Western blotting. Membranes were probed with an anti-Cdc42 antibody (Abcam).

Western immunoblotting

Cells from two-dimensional cultures were harvested in ice-cold kinase lysis buffer containing 25 mM Tris, pH 7.4, 150 mM NaCl, 5 mM EDTA, 10% glycerol, 1% Triton X-100, 10 mM β -glycerophosphate, 1 mM sodium orthovanadate, 10 mM sodium pyrophosphate, 10 μ g/ml aprotinin, and 1 mM PMSF. Cells from 3D collagen gels were harvested by brief sonication (5 s \times 3) in ice-cold lysis buffer containing 20 mM HEPES, pH 7.6, 1% Triton X-100, 150 mM NaCl, 5 mM MgCl₂, 1 mM DTT, and a protease and phosphatase inhibitor cocktail from Sigma-Aldrich. Supernatants were collected after high-speed centrifugation at 4°C. Sample protein concentration was determined using the Bradford assay (Bio-Rad), and equal amounts of protein (of 3–10 μ g) were loaded and resolved by SDS-PAGE. All membranes were blocked in 0.5% nonfat dry milk (NFDM) dissolved in 1x Tris-buffered saline/Tween-20 (TBST) except aPKC (5% BSA in TBST) for 1 h at room temperature before incubation with the appropriate primary antibody (see later

description). The secondary antibody (1:10,000) was diluted in 0.5% NFDM in 1x TBST except for PKC (5% BSA in TBST) and incubated for 1 h at room temperature. Secondary antibodies used were from Santa Cruz Biotechnology (sc-2054, goat anti-rabbit IgG-HRP; and sc-2055, goat anti-mouse IgG-HRP). Signal from the chemiluminescence substrate (NEL 100001EA; PerkinElmer, Waltham, MA) was captured using a Luminescent Image Analyzer. Membranes were incubated with primary antibody overnight at 4°C under the following conditions: anti-Nck (BD Transduction Laboratories, #610099, 1:5000; 0.5% NFDM/TBST, overnight, 4°C), anti-VE-cadherin (Bender Med System, #BMS158, 1:2500; 0.5% NFDM/TBST), anti-Cdc42 (Abcam, #ab64533, 1:250; 5% BSA/TBST), anti-aPKC (Cell Signaling, #9368, 1:500; 5% BSA/TBST), anti-phospho-aPKC (Cell Signaling, #9378, 1:1000; 0.5% NFDM/TBST), anti-glyceraldehyde-3-phosphate dehydrogenase (GAPDH; Invitrogen, #437000, 1:10,000; 0.5% NFDM/TBST), and β -actin (Sigma-Aldrich, #A1978, 1:5000; 0.5% NFDM).

Statistics

Each experiment was replicated three times. Data were analyzed using analysis of variance, followed by Tukey's multiple-comparisons test. Bar diagrams represent mean \pm SD. In box-and-whiskers plots, the central circle indicates the mean, the middle line indicates the median, and the top and bottom lines indicate the first and third quartiles, respectively. The whiskers extend up to 1.5 times the interquartile range.

ACKNOWLEDGMENTS

We thank Michiyuki Matsuda (Kyoto University, Kyoto, Japan) for the kind gift of the FRET Raichu-Cdc42 probe. We are indebted to Robert Burghardt, Director of the Image Analysis Laboratory (Texas A&M University College of Veterinary Medicine and Biomedical Sciences), for facilitating access to the imaging instrumentation. We thank Harold Ross Payne for performing transmission electron microscopy analysis. This investigation was supported by grants from the American Heart Association (12BGIA9030042 to G.M.R. and 14POST18900045 to S.P.C.) and Texas A&M University/AgriLife startup funds to G.M.R. The Image Analysis Laboratory is partly supported by the National Institutes of Health, National Center for Research Resources (1 S10 RR22532-01).

REFERENCES

- Abu Taha A, Taha M, Seebach J, Schnittler HJ (2014). ARP2/3-mediated junction-associated lamellipodia control VE-cadherin-based cell junction dynamics and maintain monolayer integrity. *Mol Biol Cell* 25, 245–256.
- Adams RH, Alitalo K (2007). Molecular regulation of angiogenesis and lymphangiogenesis. *Nat Rev Mol Cell Biol* 8, 464–478.
- Anselmi F, Orlandini M, Rocchigiani M, De Clemente C, Salameh A, Lentucci C, Oliviero S, Galvagni F (2012). c-ABL modulates MAP kinases activation downstream of VEGFR-2 signaling by direct phosphorylation of the adaptor proteins GRB2 and NCK1. *Angiogenesis* 15, 187–197.
- Aoki K, Matsuda M (2009). Visualization of small GTPase activity with fluorescence resonance energy transfer-based biosensors. *Nat Protoc* 4, 1623–1631.
- Baschieri F, Confalonieri S, Bertalot G, Di Fiore PP, Dietmaier W, Leist M, Crespo P, Macara IG, Farhan H (2014). Spatial control of Cdc42 signalling by a GM130-RasGRF complex regulates polarity and tumorigenesis. *Nat Commun* 5, 4839.
- Bayless KJ, Davis GE (2002). The Cdc42 and Rac1 GTPases are required for capillary lumen formation in three-dimensional extracellular matrices. *J Cell Sci* 115, 1123–1136.
- Bayless KJ, Johnson GA (2011). Role of the cytoskeleton in formation and maintenance of angiogenic sprouts. *J Vasc Res* 48, 369–385.
- Benard V, Bokoch GM (2002). Assay of Cdc42, Rac, and Rho GTPase activation by affinity methods. *Methods Enzymol* 345, 349–359.

- Bladt F, Aippersbach E, Gelkop S, Strasser GA, Nash P, Tafuri A, Gertler FB, Pawson T (2003). The murine Nck SH2/SH3 adaptors are important for the development of mesoderm-derived embryonic structures and for regulating the cellular actin network. *Mol Cell Biol* 23, 4586–4597.
- Boguslavsky S, Grosheva I, Landau E, Shutman M, Cohen M, Arnold K, Feinstein E, Geiger B, Bershadsky A (2007). p120 catenin regulates lamellipodial dynamics and cell adhesion in cooperation with cortactin. *Proc Natl Acad Sci USA* 104, 10882–10887.
- Buday L, Wunderlich L, Tamas P (2002). The Nck family of adapter proteins: regulators of actin cytoskeleton. *Cell Signal* 14, 723–731.
- Carmeliet P (2003). Angiogenesis in health and disease. *Nat Med* 9, 653–660.
- Chaki SP, Barhoumi R, Berginski ME, Sreenivasappa H, Trache A, Gomez SM, Rivera GM (2013). Nck enables directional cell migration through the coordination of polarized membrane protrusion with adhesion dynamics. *J Cell Sci* 126, 1637–1649.
- Cheng N, Brantley DM, Liu H, Lin Q, Enriquez M, Gale N, Yancopoulos G, Cerretti DP, Daniel TO, Chen J (2002). Blockade of EphA receptor tyrosine kinase activation inhibits vascular endothelial cell growth factor-induced angiogenesis. *Mol Cancer Res* 1, 2–11.
- Clouthier DL, Harris CN, Harris RA, Martin CE, Puri MC, Jones N (2015). requisite role for Nck adaptors in cardiovascular development, endothelial-to-mesenchymal transition, and directed cell migration. *Mol Cell Biol* 35, 1573–1587.
- Dart AE, Donnelly SK, Holden DW, Way M, Caron E (2012). Nck and Cdc42 co-operate to recruit N-WASP to promote Fc γ R-mediated phagocytosis. *J Cell Sci* 125, 2825–2830.
- Davis GE, Camarillo CW (1996). An alpha 2 beta 1 integrin-dependent pinocytic mechanism involving intracellular vacuole formation and coalescence regulates capillary lumen and tube formation in three-dimensional collagen matrix. *Exp Cell Res* 224, 39–51.
- Davis GE, Stratman AN, Sacharidou A, Koh W (2011). Molecular basis for endothelial lumen formation and tubulogenesis during vasculogenesis and angiogenic sprouting. *Int Rev Cell Mol Biol* 288, 101–165.
- Ditlev JA, Michalski PJ, Huber G, Rivera GM, Mohler WA, Loew LM, Mayer BJ (2012). Stoichiometry of Nck-dependent actin polymerization in living cells. *J Cell Biol* 197, 643–658.
- Fan X, Labrador JP, Hing H, Bashaw GJ (2003). Slit stimulation recruits Dock and Pak to the roundabout receptor and increases Rac activity to regulate axon repulsion at the CNS midline. *Neuron* 40, 113–127.
- Georgiou M, Marinari E, Burden J, Baum B (2008). Cdc42, Par6, and aPKC regulate Arp2/3-mediated endocytosis to control local adherens junction stability. *Curr Biol* 18, 1631–1638.
- Goicoechea SM, Tu Y, Hua Y, Chen K, Shen TL, Guan JL, Wu C (2002). Nck-2 interacts with focal adhesion kinase and modulates cell motility. *Int J Biochem Cell Biol* 34, 791–805.
- Good MC, Zalatan JG, Lim WA (2011). Scaffold proteins: hubs for controlling the flow of cellular information. *Science* 332, 680–686.
- Hall A (2012). Rho family GTPases. *Biochem Soc Trans* 40, 1378–1382.
- Han SP, Gambin Y, Gomez GA, Verma S, Giles N, Michael M, Wu SK, Guo Z, Johnston W, Sierecki E, et al. (2014). Cortactin scaffolds Arp2/3 and WAVE2 at the epithelial zonula adherens. *J Biol Chem* 289, 7764–7775.
- Hanajima-Ozawa M, Matsuzawa T, Fukui A, Kamitani S, Ohnishi H, Abe A, Horiguchi Y, Miyake M (2007). Enteropathogenic Escherichia coli, Shigella flexneri, and Listeria monocytogenes recruit a junctional protein, zonula occludens-1, to actin tails and pedestals. *Infect Immun* 75, 565–573.
- Herbert SP, Huiskens J, Kim TN, Feldman ME, Houseman BT, Wang RA, Shokat KM, Stainier DY (2009). Arterial-venous segregation by selective cell sprouting: an alternative mode of blood vessel formation. *Science* 326, 294–298.
- Herwig L, Blum Y, Krudewig A, Ellerstsdottir E, Lenard A, Belting HG, Affolter M (2011). Distinct cellular mechanisms of blood vessel fusion in the zebrafish embryo. *Curr Biol* 21, 1942–1948.
- Hirata E, Yukinaga H, Kamioka Y, Arakawa Y, Miyamoto S, Okada T, Sahai E, Matsuda M (2012). In vivo fluorescence resonance energy transfer imaging reveals differential activation of Rho-family GTPases in glioblastoma cell invasion. *J Cell Sci* 125, 858–868.
- Humphries AC, Donnelly SK, Way M (2014). Cdc42 and the Rho GEF intersectin-1 collaborate with Nck to promote N-WASP-dependent actin polymerisation. *J Cell Sci* 127, 673–685.
- Iruela-Arispe ML, Davis GE (2009). Cellular and molecular mechanisms of vascular lumen formation. *Dev Cell* 16, 222–231.
- Itoh M, Nagafuchi A, Moroi S, Tsukita S (1997). Involvement of ZO-1 in cadherin-based cell adhesion through its direct binding to alpha catenin and actin filaments. *J Cell Biol* 138, 181–192.
- Jeltsch M, Leppanen VM, Saharinen P, Alitalo K (2013). Receptor tyrosine kinase-mediated angiogenesis. *Cold Spring Harb Perspect Biol* 5, a009183.
- Jin Y, Liu Y, Lin Q, Li J, Druso JE, Antonyak MA, Meininger CJ, Zhang SL, Dostal DE, Guan JL, et al. (2013). Deletion of Cdc42 enhances ADAM17-mediated vascular endothelial growth factor receptor 2 shedding and impairs vascular endothelial cell survival and vasculogenesis. *Proc Natl Acad Sci USA* 110, 4181–4197.
- Kamei M, Saunders WB, Bayless KJ, Dye L, Davis GE, Weinstein BM (2006). Endothelial tubes assemble from intracellular vacuoles in vivo. *Nature* 442, 453–456.
- Kim DJ, Martinez-Lemus LA, Davis GE (2013). EB1, p150Glued, and Clasp1 control endothelial tubulogenesis through microtubule assembly, acetylation, and apical polarization. *Blood* 121, 3521–3530.
- Kiosses WB, Hood J, Yang S, Gerritsen ME, Cheresh DA, Alderson N, Schwartz MA (2002). A dominant-negative p65 PAK peptide inhibits angiogenesis. *Circ Res* 90, 697–702.
- Koh W, Mahan RD, Davis GE (2008a). Cdc42- and Rac1-mediated endothelial lumen formation requires Pak2, Pak4 and Par3, and PKC-dependent signaling. *J Cell Sci* 121, 989–1001.
- Koh W, Stratman AN, Sacharidou A, Davis GE (2008b). In vitro three dimensional collagen matrix models of endothelial lumen formation during vasculogenesis and angiogenesis. *Methods Enzymol* 443, 83–101.
- Kovacs EM, Verma S, Ali RG, Ratheesh A, Hamilton NA, Akhmanova A, Yap AS (2011). N-WASP regulates the epithelial junctional actin cytoskeleton through a non-canonical post-nucleation pathway. *Nat Cell Biol* 13, 934–943.
- Kutys ML, Yamada KM (2014). An extracellular-matrix-specific GEF-GAP interaction regulates Rho GTPase crosstalk for 3D collagen migration. *Nat Cell Biol* 16, 909–917.
- Lamalice L, Houle F, Huot J (2006). Phosphorylation of Tyr1214 within VEGFR-2 triggers the recruitment of Nck and activation of Fyn leading to SAPK2/p38 activation and endothelial cell migration in response to VEGF. *J Biol Chem* 281, 34009–34020.
- Lamalice L, Le Boeuf F, Huot J (2007). Endothelial cell migration during angiogenesis. *Circ Res* 100, 782–794.
- Lampugnani MG, Orsenigo F, Rudini N, Maddaluno L, Boulday G, Chapon F, Dejana E (2010). CCM1 regulates vascular-lumen organization by inducing endothelial polarity. *J Cell Sci* 123, 1073–1080.
- Li W, Fan J, Woodley DT (2001). Nck/Dock: an adapter between cell surface receptors and the actin cytoskeleton. *Oncogene* 20, 6403–6417.
- Li X, Meriane M, Triki I, Shekarabi M, Kennedy TE, Larose L, Lamarche-Vane N (2002). The adaptor protein Nck-1 couples the netrin-1 receptor DCC (deleted in colorectal cancer) to the activation of the small GTPase Rac1 through an atypical mechanism. *J Biol Chem* 277, 37788–37797.
- Liu Y, Jin Y, Li J, Seto E, Kuo E, Yu W, Schwartz RJ, Blazo M, Zhang SL, Peng X (2013). Inactivation of Cdc42 in neural crest cells causes craniofacial and cardiovascular morphogenesis defects. *Dev Biol* 383, 239–252.
- Lockwood C, Zaidel-Bar R, Hardin J (2008). The *C. elegans* zonula occludens ortholog cooperates with the cadherin complex to recruit actin during morphogenesis. *Curr Biol* 18, 1333–1337.
- Machida K, Mayer BJ (2005). The SH2 domain: versatile signaling module and pharmaceutical target. *Biochim Biophys Acta* 1747, 1–25.
- Miura K, Nam JM, Kojima C, Mochizuki N, Sabe H (2009). EphA2 engages Git1 to suppress Arf6 activity modulating epithelial cell-cell contacts. *Mol Biol Cell* 20, 1949–1959.
- Montero-Balaguer M, Swirsding K, Orsenigo F, Cotelli F, Mione M, Dejana E (2009). Stable vascular connections and remodeling require full expression of VE-cadherin in zebrafish embryos. *PLoS One* 4, e5772.
- Pawson T (2007). Dynamic control of signaling by modular adaptor proteins. *Curr Opin Cell Biol* 19, 112–116.
- Qi Y, Liu J, Wu X, Brakebusch C, Leitges M, Han Y, Corbett SA, Lowry SF, Graham AM, Li S (2011). Cdc42 controls vascular network assembly through protein kinase Ciota during embryonic vasculogenesis. *Arterioscler Thromb Vasc Biol* 31, 1861–1870.
- Rajput C, Kini V, Smith M, Yazbeck P, Chavez A, Schmidt T, Zhang W, Knezevic N, Komarova Y, Mehta D (2013). Neural Wiskott-Aldrich syndrome protein (N-WASP)-mediated p120-catenin interaction with Arp2-Actin complex stabilizes endothelial adherens junctions. *J Biol Chem* 288, 4241–4250.
- Rivera GM, Briceno CA, Takeshima F, Snapper SB, Mayer BJ (2004). Inducible clustering of membrane-targeted SH3 domains of the adaptor protein Nck triggers localized actin polymerization. *Curr Biol* 14, 11–22.

- Rodriguez-Boulan E, Macara IG (2014). Organization and execution of the epithelial polarity programme. *Nat Rev Mol Cell Biol* 15, 225–242.
- Roignot J, Peng X, Mostov K (2013). Polarity in mammalian epithelial morphogenesis. *Cold Spring Harb Perspect Biol* 5, a013789.
- Rosse C, Linch M, Kermorgant S, Cameron AJ, Boeckeler K, Parker PJ (2010). PKC and the control of localized signal dynamics. *Nat Rev Mol Cell Biol* 11, 103–112.
- Sauteur L, Krudewig A, Herwig L, Ehrenfeuchter N, Lenard A, Affolter M, Belting HG (2014). Cdh5/VE-cadherin promotes endothelial cell interface elongation via cortical actin polymerization during angiogenic sprouting. *Cell Rep* 9, 504–513.
- Sigurbjornsdottir S, Mathew R, Leptin M (2014). Molecular mechanisms of de novo lumen formation. *Nat Rev Mol Cell Biol* 15, 665–676.
- Stoletov KV, Ratcliffe KE, Spring SC, Terman BI (2001). NCK and PAK participate in the signaling pathway by which vascular endothelial growth factor stimulates the assembly of focal adhesions. *J Biol Chem* 276, 22748–22755.
- Strilic B, Kucera T, Eglinger J, Hughes MR, McNagny KM, Tsukita S, Dejana E, Ferrara N, Lammert E (2009). The molecular basis of vascular lumen formation in the developing mouse aorta. *Dev Cell* 17, 505–515.
- Tehrani S, Tomasevic N, Weed S, Sakowicz R, Cooper JA (2007). Src phosphorylation of cortactin enhances actin assembly. *Proc Natl Acad Sci USA* 104, 11933–11938.
- Tu Y, Li F, Wu C (1998). Nck-2, a novel Src homology2/3-containing adaptor protein that interacts with the LIM-only protein PINCH and components of growth factor receptor kinase-signaling pathways. *Mol Biol Cell* 9, 3367–3382.
- Vaynberg J, Fukuda T, Chen K, Vinogradova O, Velyvis A, Tu Y, Ng L, Wu C, Qin J (2005). Structure of an ultraweak protein-protein complex and its crucial role in regulation of cell morphology and motility. *Mol Cell* 17, 513–523.
- Weber GF, Bjerke MA, DeSimone DW (2011). Integrins and cadherins join forces to form adhesive networks. *J Cell Sci* 124, 1183–1193.
- Weis SM, Cheresh DA (2011). Tumor angiogenesis: molecular pathways and therapeutic targets. *Nat Med* 17, 1359–1370.
- Yamamoto H, Ehling M, Kato K, Kanai K, van Lessen M, Frye M, Zeuschner D, Nakayama M, Vestweber D, Adams RH (2015). Integrin beta1 controls VE-cadherin localization and blood vessel stability. *Nat Commun* 6, 6429.
- Zandy NL, Playford M, Pendergast AM (2007). Abl tyrosine kinases regulate cell-cell adhesion through Rho GTPases. *Proc Natl Acad Sci USA* 104, 17686–17691.
- Zovein AC, Luque A, Turlo KA, Hofmann JJ, Yee KM, Becker MS, Fassler R, Mellman I, Lane TF, Iruela-Arispe ML (2010). Beta1 integrin establishes endothelial cell polarity and arteriolar lumen formation via a Par3-dependent mechanism. *Dev Cell* 18, 39–51.